AADE-17-NTCE-095

Choke Controller Design for Automated Managed Pressure Drilling with Realistic Operational System Conditions

Adrian Ambrus, Ali Karimi Vajargah*, Pradeepkumar Ashok and Eric van Oort, The University of Texas at Austin

*Now with Quantum Reservoir Impact

Abstract

Managed Pressure Drilling (MPD) techniques offer great promise for improving rig safety and reducing non-productive time when drilling wells with narrow drilling margins. However, only a few MPD solutions take into account the complex pressure dynamics in the wellbore, particularly when two-phase flow conditions are present, such as during dynamic well control situations with gas kicks. In addition, it is also desired to use a robust MPD control algorithm that can handle ideal as well as degraded system conditions.

In this paper, we develop an MPD choke control algorithm based on a simplified transient hydraulic model capable of handling both single- and two-phase flow. A Bayesian network is used to detect a variety of events leading to degraded system conditions, and subsequently adjust the control response and the process model to accommodate such conditions. The effectiveness of the proposed algorithm is evaluated through simulations of various test cases conducted with an advanced multi-phase software package.

The simulation results show that the choke control algorithm successfully responds to kick, lost circulation, and a variety of other incidents that may occur during MPD operations. In addition, it has been shown that the control system can detect induced system faults and update the model in a timely manner. The developed choke control algorithm, in association with the advanced event detection system provide a powerful tool for automated MPD control.

1. Introduction

As more wells are being drilled in areas with increasingly complex pressure windows, keeping the annular pressure within narrow margins defined by the formation pore pressure (or wellbore collapse pressure, whichever of the two is higher), and fracture pressure, becomes a challenging drilling automation task. Managed Pressure Drilling (MPD) offers a solution to this problem, enabling precise control of annular pressure profiles. MPD technologies include the Constant Bottom-Hole Pressure (CBHP) Method, the Continuous Circulation Method (CCM). , Mud Cap Drilling (Pressurized (PMCD) or Floating (FMCD)), Dual Gradient Drilling including Subsea Mud Lift Drilling, etc. Among these, the CBHP method has seen the most development and application in recent years. In a CBHP-controlled well, the annulus is sealed at all times by a rotating control device (RCD) mounted above the conventional blow-out preventers. The return flow is diverted through a choke manifold with adjustable chokes that trap or release back-pressure in the well. Several control systems for CBHP MPD using automated chokes have been developed (Santos et al., 2003; van Riet et al., 2003; Saeed et al., 2012).

Several important items need to be addressed when designing control systems for CBHP MPD. The bandwidth of the physical system varies with scale, ranging from shallow wells to deep and Extended Reach Drilling (ERD) wells. As the measured depth of the well increases, so does travel time for pressure waves generated at the surface (standpipe or choke) to reach the bottom of the well, which reduces the control performance, and may even cause large pressure fluctuation and potential instability. This situation is further complicated when gas is present in the well, as the compressibility of a gas-liquid mixture tends to be significantly higher than that of a pure liquid, even at low gas volumes (Kaasa et al, 2012). This makes pressure control during a gas kick event even more challenging, particularly when previously dissolved gas breaks out of the drilling mud, and the resulting free gas rapidly expands as it reaches the surface.

The control bandwidth is further limited by the choke closing and opening time, and also by the flow rate through the choke (Godhavn, 2010). The controller needs to handle both high and low flow rates, such as the slow circulation rates used in well control. During pipe tripping and connections, an additional back-pressure pump or flow diverter may be used to provide continuous flow through the choke. In such cases, precise coordination between pump and choke control modules is crucial to achieve the desired pressure response with minimal overshoot or undershoot. In addition, the controller needs to handle external disturbances, such as hoisting and lowering of the drill string, or heave motion, on floating off-shore rigs. A robust control system needs to accommodate various contingency scenarios and non-ideal operating conditions, starting with kicks and loss of drilling fluid, and continuing with plugged or washed out choke valves or bit nozzles, pump degradation and failure, leaks ("washouts") in the drill string, annulus pack-offs due to cuttings build-up, borehole enlargement, etc. (Guner, 2009).

In this paper, we present an approach for designing model-based choke control algorithms that include robustness to system faults and disturbances, as well as logic for detecting and accommodating a variety of events. The algorithms and methods used are tested using a state-of-the-art multi-phase hydraulics simulator capable of generating various operating conditions.

2. System Design

We approach the control design problem through a modular structure, which performs several tasks concurrently at a system update rate of 1 Hz or better. Real-time measurements (flow rates, pressures, mud volumes) are communicated to the controllers, observers and event detection algorithms. The observers estimate key parameters which are subsequently fed to a hydraulics model, responsible for providing the control set points. From these set points, the required choke adjustment is calculated using a choke model. The control logic switches whenever certain events are detected. **Figure 1** shows a high-level block diagram of the system, with the relevant inputs and outputs for the different components, to be detailed in the following sections.

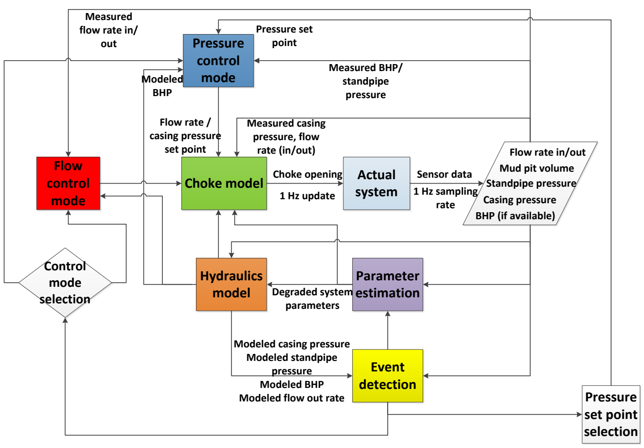

Figure 1. System Block Diagram.

2.1 Hydraulics Model

The system uses a simplified transient hydraulics model, based on a reduced Drift-Flux approach (Aarsnes et al., 2016a; Ambrus et al., 2015). The model consists of a set of ordinary differential equations governing the pressure dynamics in the well, and a partial differential equation for gas-liquid dynamics, essential for modeling two-phase scenarios such as gas influx. The model calculates pressures at various locations (well head, bottom-hole, standpipe etc.), along with real-time gas/liquid distributions and velocities along the well. An explicit finite difference numerical scheme is used to solve the model equations in real time, and the model inputs are continuously updated as new measurements become available.

2.2 Choke Model

A simple choke model is used to automatically compute the choke position adjustment in response to a change in pressure or flow rate set point. The model, capable of handling both single- and two-phase flow, can be formulated, for a mixed (gas-liquid) flow regime, as (Ma et al., 2016):

$$q_c = C_v Z \left(\frac{x_l}{\rho_l} + \frac{x_g}{\rho_g}\right) \sqrt{\frac{p_c - p_s}{x_l/\rho_l + x_g/(Y^2 \rho_g)}} \tag{1}$$

where q_c is the total volume flow rate through the choke, ρ_l and ρ_g are liquid and gas density at the choke, x_l and x_g are the liquid and gas mass flow fraction through the choke, p_c is the surface back-pressure, p_s is the pressure downstream of the choke (either mud gas separator or atmospheric pressure), C_v is a constant related to the choke orifice area, Y is a factor accounting for gas expansion, and Z is the choke opening.

2.3 Choke Controller

The choke controller is designed to operate in two modes, based on the system state:

- **Pressure control mode**: this is the default mode, and it is used during most operations, including influx circulation once the well is overbalanced. The pressure control law is designed to minimize the error in tracking a downhole or standpipe pressure set point (e_p), while accounting for any disturbances to the system, such as a change in circulation rate, or expansion of a gas kick. The control law consists of two layers: first, a flow rate or casing pressure (back-pressure) set point is computed, from which the updated choke opening is calculated using the choke model from Eq. 1. If a flow rate set point is used, the control law may be expressed as:

$$Z = \frac{q_{l,out}^{sp}}{C_v \sqrt{p_c - p_s}} \frac{\rho_l}{\chi_l} \sqrt{\frac{\chi_l}{\rho_l} + \frac{\chi_g}{Y^2 \rho_g}} \tag{2}$$

$$q_{l,out}^{sp} = \frac{V_a}{\beta}\left(k_P e_p + k_I \int e_p\right) + q_{l,in} - q_{g,out} + q_{g,ex} \tag{3}$$

where $q_{l,out}^{sp}$ is the flow rate out set point, V_a is the annular volume, β is the drilling fluid bulk modulus, $q_{l,in}$ is the liquid injection rate (either from the main pump, or an auxiliary/back-pressure pump), $q_{g,out}$ is gas flow out of the well, and $q_{g,ex}$ is the rate of volumetric gas expansion inside the well (computed by the reduced Drift-Flux model). The constants k_P and k_I are controller gains. A more robust control law may also be derived through advanced control techniques, such as gain scheduling and convex optimization (Aarsnes et al., 2016b). This control law uses a linearized model and is optimized for a range of uncertainty bounds to compute a back-pressure set point which translates to the desired BHP. The choke adjustment is then computed for this back-pressure set point from Eq. 1.

- **Flow control mode**: used to limit an active influx or mud loss to the formation. The control law in this case uses the same choke model to open or close the choke so as to balance the flow out with the flow in from the mud pump. This may account for gas expansion ($q_{g,ex}$) and gas flow out ($q_{g,out}$) if gas has already reached the surface.

$$Z = \frac{q_{l,in} + q_{g,ex} - q_{g,out}}{C_v\sqrt{p_c - p_s}} \frac{\rho_l}{\chi_l}\sqrt{\frac{\chi_l}{\rho_l} + \frac{\chi_g}{Y^2\rho_g}} \tag{4}$$

Switching between the two modes needs to be done smoothly to avoid chattering in the actuator signal, for instance by applying a smoothing function or low-pass filter.

2.4 Pressure Set Point Selection

For the pressure control mode, the tracking error, e_p, can be defined as the instantaneous difference between the measured pressure (BHP or standpipe) and the set point. The choice of which set point to use depends on whether a downhole pressure sensor is available or not. In the latter case, the standpipe pressure will be used instead. One disadvantage to using standpipe pressure is that is very sensitive to any changes in flow rate, and also to the presence of drill string leaks (washouts), plugged or washed out bit nozzles, or to a loss in pump efficiency. BHP measurements, on the other hand, can have a substantial lag and/or low sampling rates, based on the telemetry method used. So the control system may often face a situation where it will have to quickly update the pressure set point, and additional logic needs to be implemented to ensure a seamless transition.

When a kick or lost circulation event is detected, the set point needs to be updated to ensure that no further influx or loss occurs (unless drilling in naturally fractured formations where losses are inevitable but can be minimized). This is done by adding a safety margin above (for influx) or below (for loss) the measured or modeled downhole pressure and using that as the new set point. Updating the set point should be done carefully, since sudden changes in the set point may cause the controller to overshoot. For this purpose, a low-pass filter with a 30 second time constant is applied to the set point, and this filtered value is used by the controller.

2.5 Event Detection

The system uses a Bayesian Network, which is a type of probabilistic graphical model, widely used in statistical computing and pattern recognition applications (Koller and Friedman, 2009). The network is designed as a Naïve Bayes model, where a class variable, whose outcomes represent a set of possible events, is linked to several conditionally independent feature variables (**Figure 2**). The links between the nodes are mathematically represented by conditional probability tables (CPTs). Each CPT can be assigned, e.g. by a domain expert, or learned from labeled data sets. The features represent sensor data such as pressures, flow rates, pit volume, and their respective trends. Each of these nodes can be characterized by a set of discrete states, for instance constant/increasing/decreasing for trend-based variables, or low/normal/high for location-based features (the classification can be based on hard thresholds or fuzzy intervals). Some of the nodes relate a measured variable to a model-predicted value (e.g. pump pressure, casing pressure). Two special nodes designating the pump status (pumps off, pumps ramping up/down, or at steady state), and well control status (overbalanced/underbalanced) are also included to provide additional contextual information to the detection algorithm. The nodes are continuously updated as new information is available, and the Event variable is then evaluated using probabilistic inference, resulting in a probability of each of the possible outcomes. The probabilistic nature of the model allows for incorporation of uncertainty, through the CPT definitions. In the current work, the following events are modeled: kick, lost circulation, pump efficiency loss, plugged bit nozzle, plugged choke, and drill string washout.

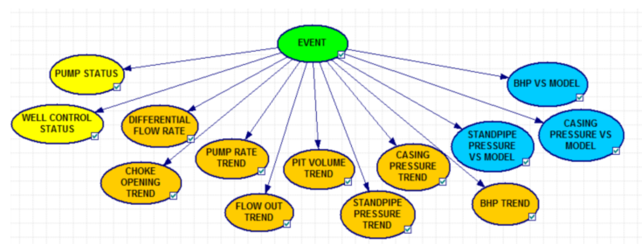

Figure 2. Bayesian Network for event detection.

2.6 Parameter Estimation

Aside from event detection, the control system includes real-time estimation algorithms for learning degraded system parameters, and also for monitoring external disturbances (influx or mud loss), or parameters related to the formation (like pore pressure and fracture pressure). Combining real-time data with model-based estimation techniques helps maximize the amount of information gained during a fault in the process. This offers an alternative to existing industry practices, such as formation pressure tests/leak-off tests which can often prove to be time-consuming or difficult to interpret.

The influx and mud loss rate is calculated from the annular pressure dynamics, to which a low-pass filter $\mathcal{F}$ is applied:

$$q_{kick/loss} = \frac{V_a}{\beta}\,\mathcal{F}\left\{\dot{p}_c - \frac{\beta}{V_a}\left(q_{l,in} - q_{l,out} + q_{g,ex}\right)\right\} \tag{5}$$

Then, the calculated rates can be used to back-calculate the reservoir pore pressure and fracture pressure, using a reservoir model and a fluid loss model (for instance, a production/loss index multiplied by a pressure draw-down). Recursive Least Squares estimation is used to update these in real time (see Aarsnes et al. (2015), Ambrus et al. (2016) for further details).

Other parameters monitored include choke orifice area, bit nozzle area, and mud pump volumetric efficiency. These are modeled using a set of non-linear observers, formulated using a simplified version of the hydraulics model. For the choke area estimation, we will use a first-order ordinary differential equation of the annular pressure dynamics (Eq. 6) coupled with a first-order parameter update law (Eq. 7):

$$\frac{d\hat{p}_c}{dt} = \frac{\beta}{V_a}\left[q_{l,in} - \frac{\hat{A}_c\sqrt{2(\hat{p}_c - p_s)}}{\sqrt{\rho_l}}Z\right] + \lambda_1(p_c - \hat{p}_c) \tag{6}$$

$$\frac{d\hat{A}_c}{dt} = -\frac{1}{\gamma_1}\frac{\beta}{V_a}\frac{Z\sqrt{2(\hat{p}_c - p_s)}}{\sqrt{\rho_l}}(p_c - \hat{p}_c) \tag{7}$$

where $\hat{A}_c$ is the estimated choke area, $\hat{p}_c$ is the estimated back-pressure, p_c is the measured back-pressure, and λ_1, γ_1 are tuning parameters affecting the observer convergence. For the bit nozzle area, we use the following equations:

$$\frac{d\hat{q}_b}{dt} = \frac{1}{M}(p_{st} - p_f + p_g - p_c - \frac{\rho_l}{2}\hat{C}_b\hat{q}_b^2) + \lambda_2(q_{l,in} - \hat{q}_b) \tag{8}$$

$$\frac{d\hat{C}_b}{dt} = -\gamma_2\frac{\rho_l}{2M}\hat{q}_b^2(q_{l,in} - \hat{q}_b) \tag{9}$$

where $\hat{C}_b$ is a factor equal to the inverse of nozzle area squared, $\hat{q}_b$ is estimated flow rate through the drill bit, p_{st} is the standpipe pressure, p_f is frictional pressure drop, p_g is hydrostatic pressure, and M is fluid inertia. p_f can be calculated using correlations for yield-power law fluids (Ahmed and Miska, 2009). Tuning parameters λ_2 and γ_2 are used to calibrate the estimation law. Finally, the mud pump efficiency estimation is given by:

$$\frac{d\hat{p}_c}{dt} = \frac{\beta}{V_a}(\hat{\eta}q_{l.in} - q_c) + \lambda_3(p_c - \hat{p}_c) \tag{10}$$

$$\frac{d\hat{\eta}}{dt} = -\frac{1}{\gamma_3}\frac{\beta}{V_a}q_{l.in}(p_c - \hat{p}_c) \tag{11}$$

where $\hat{\eta}$ is the estimate of mud pump volumetric efficiency, and λ_3 and γ_3 are tuning parameters.

3. Simulation Case Setup

The control system introduced in Section 2 will be demonstrated in a series of simulations conducted with an advanced multi-phase hydraulics simulator (Ma et al., 2016). The test setup is that of a 15,850-ft MD well with a deviated trajectory shown in **Figure 3**, with 9.76-in (inner diameter) casing set at 13,000 ft and a 9.5-in open-hole diameter.

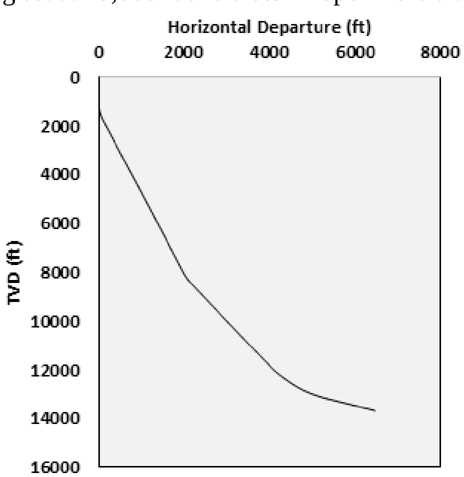

Figure 3. Well trajectory for simulation case.

The drill string consists of drill pipe with 5-in OD, 4.28-in ID and a 1285-ft bottom-hole assembly comprising 6.5-in OD, 2.5-in ID drill collars. A synthetic-based mud with an oil/water ratio of 70/30 is used. The mud properties and other parameters are given in **Table 1**, while **Figure 4** shows the formation pressure window.

Table 1. Simulation Parameters.

Property	Value	Unit
Mud weight	10	ppg
Plastic viscosity	20	cP
Yield stress	10	lbs/(100ft^2)
Number and size of bit nozzles	3x0.5	in
Bit nozzle total flow area	0.6	in^2
Choke line ID	2	in
Circulation rate	600	gpm
Gas viscosity	0.005	cP
Gas specific gravity	0.65	-
Gas adiabatic index	1.32	-
Pore pressure at bottom-hole	7000	psi
Fracture initiation / propagation pressure at casing shoe	7200/ 7000	psi
Gas production index	10^{-8}	m^3/s/Pa
Mud loss index	10^{-9}	m^3/s/Pa
Surface temperature	60	°F
Bottom-hole temperature	135	°F

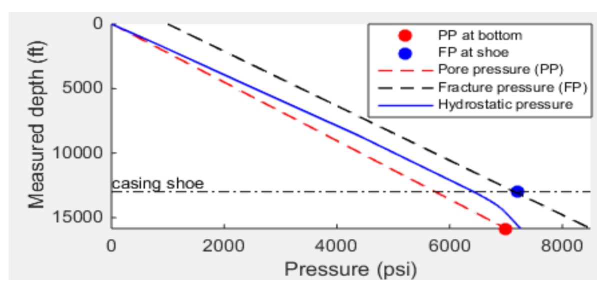

Figure 4. Pressure window for simulation case.

The measurements available in the simulations include standpipe pressure, well head pressure, pump rate, flow rate out, and pit volume. The BHP sensor is not available, and thus the system needs to rely on the modeled BHP (or the standpipe pressure, if no event occurs that would complicate control using the reading from the standpipe). Random noise with a standard deviation of 30 psi is added to the pressure readings, while flow rate and pit volume are injected with noise equal to 5% of the reading for flow rate, and 1% for pit volume.

Seven distinct scenarios are generated to evaluate the controller performance: kick, lost circulation, plugged choke, plugged bit nozzle, loss of pump efficiency, drill pipe washout, and BHP control during a drill pipe connection. In each of these we will evaluate the control response, event detection accuracy, and parameter estimation. An event detection threshold of 50% is used throughout the simulations.

4. Simulation Results

This section details the simulation scenarios and presents the relevant outputs (pressure trends, choke opening, flow rate, pit gain, event detection, and parameter estimation results), for each of these cases, together with a discussion of the results.

4.1 Kick Handling

This scenario starts with the well at overbalance. After 5 minutes, an over-pressured dry gas reservoir with a pore pressure of 7870 psi is drilled through, resulting in an underbalance of 300 psi at the well bottom. The system manages to detect the kick after a pit gain of less than 1 bbl, as the kick event probability reaches close to 100% (**Figure 5).** The controller immediately proceeds to close the choke in flow control mode, until the influx stops, about 8 minutes later. During this process, an additional 1 bbl of pit gain is observed. However, it should be noted that at this point the gas is fully dissolved in the mud. While the kick is being attenuated by rapidly closing the choke, the system also estimates the reservoir pressure, and the influx rate (**Figure 6**), from which the production index can also be inferred. The kick response time can be reduced by adjusting the controller aggressiveness, but this may affect the estimation of reservoir pressure as it may not have sufficient data samples to learn from. Depending on the kick size and detection volume, however, it may be preferred to minimize response times.

Once no further influx is detected, the system switches to pressure control with a set point equal to the estimated reservoir pressure plus a safety margin of 150 psi. The controller manages to keep BHP within 50 psi of the target, even when gas breaks out of the solution, as seen by the increased pit gain and flow out at 70 minutes (see **Figure 7** and **Figure 8**). As the gas expands near the top of the well, the choke opening is quickly adjusted, resulting in a noisy pattern in flow out, but the BHP signature remains smooth. The close agreement between the BHP predicted by the model and the actual value should also be noted, which indicates that the model is also correct in tracking the amount of gas once it starts breaking out of the mud.

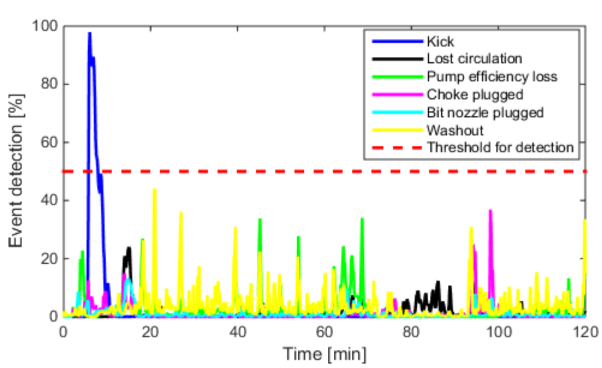

Figure 5. Event detection outputs for kick scenario.

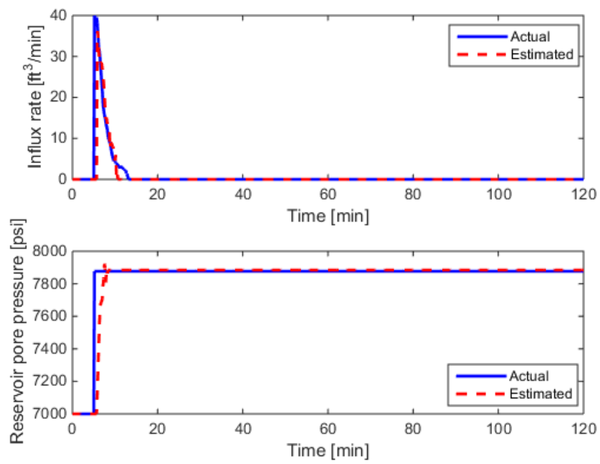

Figure 6. Influx rate and pore pressure.

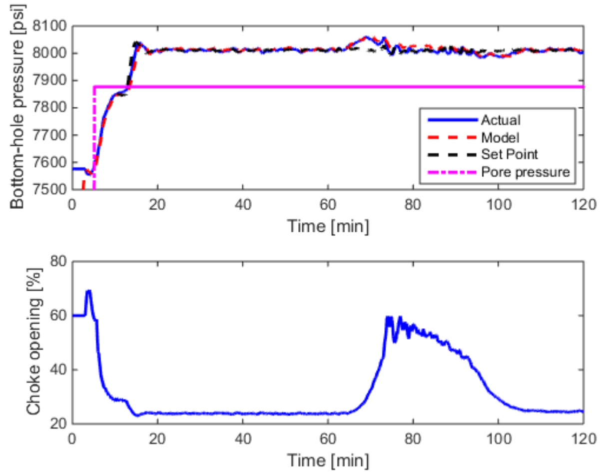

Figure 7. Bottom-hole pressure and choke opening for kick scenario.

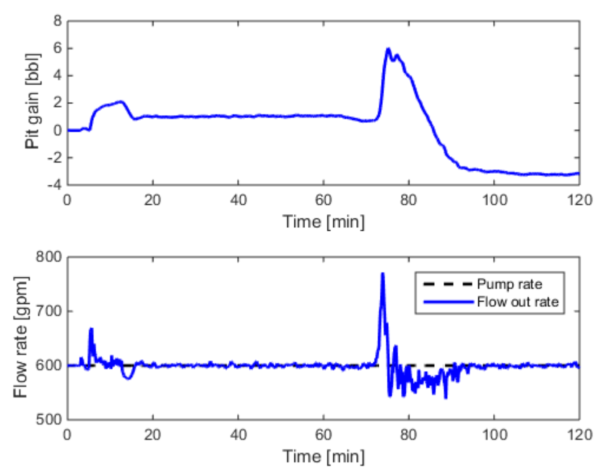

Figure 8. Pit gain/loss and flow rates for kick scenario.

4.2 Lost Circulation

This simulation begins with a circulation rate of 400 gpm, which results in a casing shoe pressure well below the fracture initiation pressure. At 5 minutes, the pump is ramped up to 600 gpm, resulting in the circulating pressure to exceed the limit for fracture initiation. As the fracture is opened, mud starts flowing into the formation, and close to 1 bbl of mud over 1 minute is lost before the system detects the loss event with a probability of 70% (**Figure 9**). Note that the total loss at this point is 5 bbl, however this includes any temporary losses caused by the change in pump rate, as the flow out lags behind the pump rate due to mud compressibility.

Upon detection, the system initiates the flow control, opening the choke to release back-pressure. It takes about 7 minutes to stop the loss, during which time the system keeps track of the loss rate and estimates the fracture pressure (the estimate falls between the fracture initiation and propagation pressure, as shown in **Figure 10**). The system then applies a new pressure set point below the fracture propagation pressure (which, in this case, was assumed to be below the initiation pressure) to ensure that no further mud losses occur. The pressure and flow trends throughout the incident are shown in **Figure 11** and **Figure 12**. The increased flow out after 15 minutes is a result of some of the mud flowing back to the well as the fracture is closed. The event detection is able to correctly distinguish this from a kick, recognizing that a loss event had just occurred.

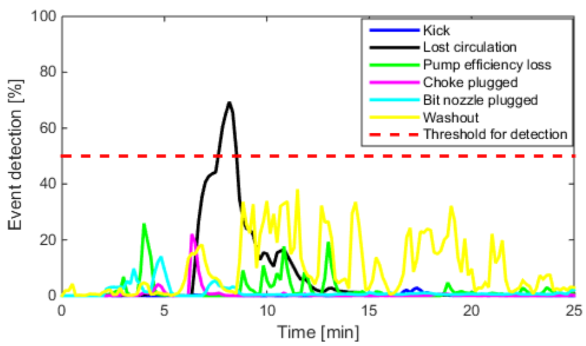

Figure 9. Event detection outputs for lost circulation scenario.

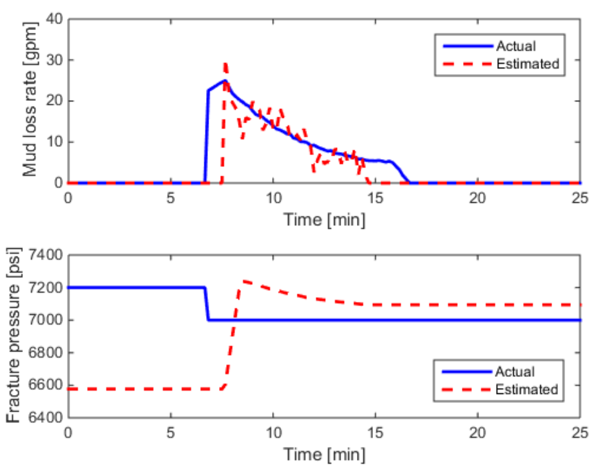

Figure 10. Lost circulation rate and fracture pressure at casing shoe.

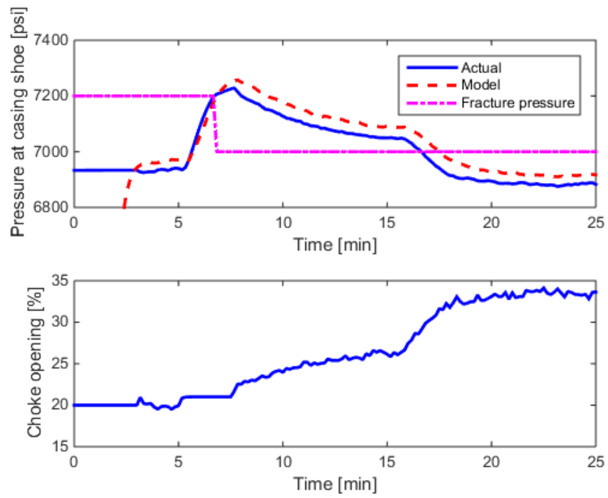

Figure 11. Casing shoe pressure and choke opening for lost circulation scenario.

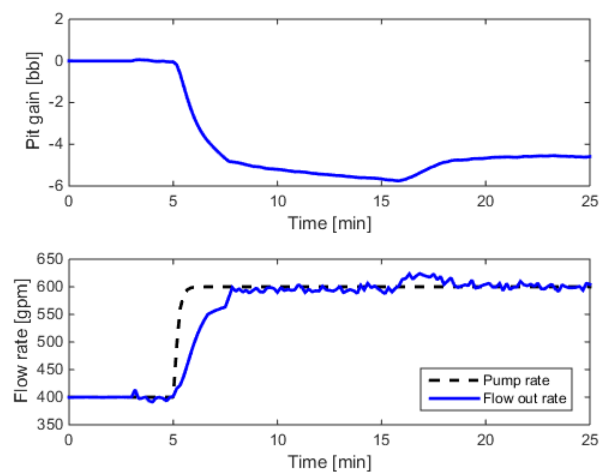

Figure 12. Pit gain/loss and flow rates for lost circulation scenario.

4.3 Plugged Choke Valve

A partially plugged choke (e.g. due to solid debris or large cavings) is simulated by reducing the effective flow area by 30%. While plugging the choke may happen gradually, the reduction is assumed to be instantaneous here, to test the controller robustness when dealing with a sudden fault. The plug starts at 15 minutes and is quickly detected with a 90% probability after less than 1 minute, as shown in **Figure 13**. As the choke gets plugged, the choke needs to open quickly to counter the increase in back-pressure. The system is able to quickly learn the change in choke area due to the plug, and apply a lower choke opening until the pressure stabilizes (see **Figure 14** and **Figure 15**). When the plug is removed (again, assuming an instantaneous change), 10 minutes later, the choke needs to be again closed to restore the BHP to the value prior to the incident. It should be noted that failure to update the choke area used in the control model quickly enough would result in too much or too little back-pressure being applied, causing potential fracturing or underbalanced situations. It should be noted that while the plug is still present, the detection probability is quickly reduced, because the model is now updated with the correct choke area. There is another spike in detection once the choke plug is removed, which is quickly damped as soon as the choke area communicated to the model is correctly updated once again.

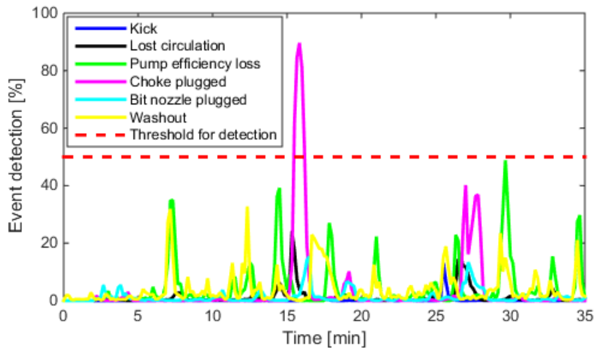

Figure 13. Event detection outputs for plugged choke scenario.

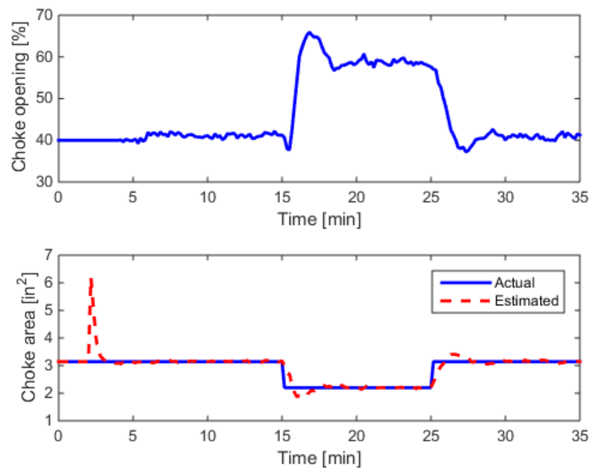

Figure 14. Choke opening and choke orifice area for plugged choke scenario.

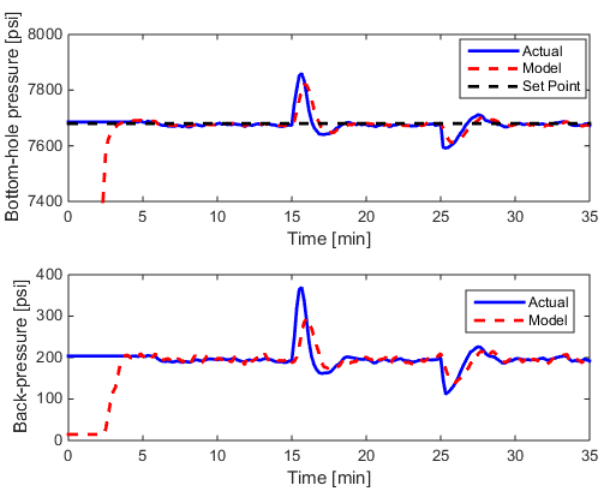

Figure 15. Bottom-hole pressure and back-pressure for plugged choke scenario.

4.4 Plugged Bit Nozzle

In this simulation, one of the three 0.5-inch bit nozzles becomes suddenly plugged at 15 minutes, which is almost immediately caught by the event detection with a probability close to 80%, as indicated by **Figure 16**. This presents a challenge to the pressure controller, because it is initially set to use standpipe pressure feedback, and once the nozzle is plugged, the higher bit pressure drop makes the standpipe pressure increase significantly (lower plot of **Figure 17**), and the controller, unless instructed otherwise, will open the choke to offset that increase in pump pressure. Naturally, this causes a drop in BHP (upper plot of **Figure 17**), which could jeopardize well control if the margins are very tight. The system remedies this problem, as soon as the plug is detected, by switching the pressure control set point from standpipe to BHP. In the absence of a downhole sensor, the controller will rely on the value from the hydraulics model, which stays close to the actual value throughout the incident. In addition, the system successfully estimates the new bit flow area and proceeds to close the choke, restoring the BHP to its value prior to the incident **(Figure 18**). If downhole pressure data were available, the BHP set point could have been used throughout to avoid this issue. However, this simulation shows that the system is capable of handling such a scenario just with surface data and a properly calibrated hydraulics model.

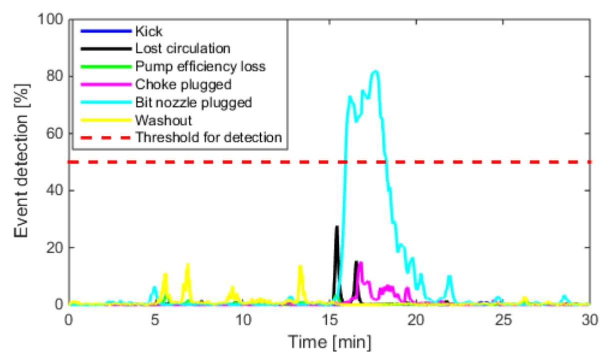

Figure 16. Event detection outputs for plugged nozzle scenario.

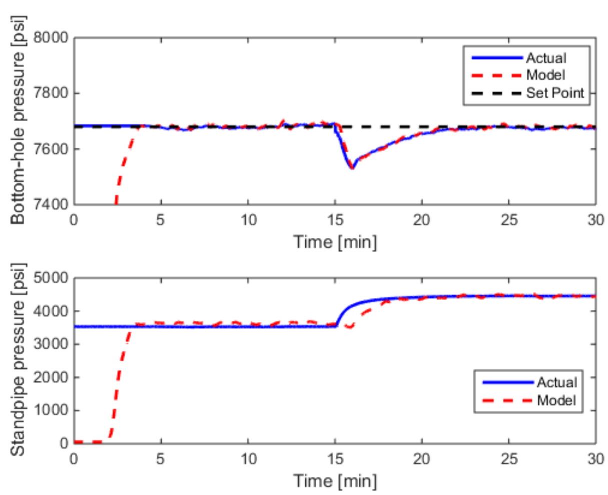

Figure 17. Bottom-hole pressure and standpipe pressure for plugged nozzle scenario.

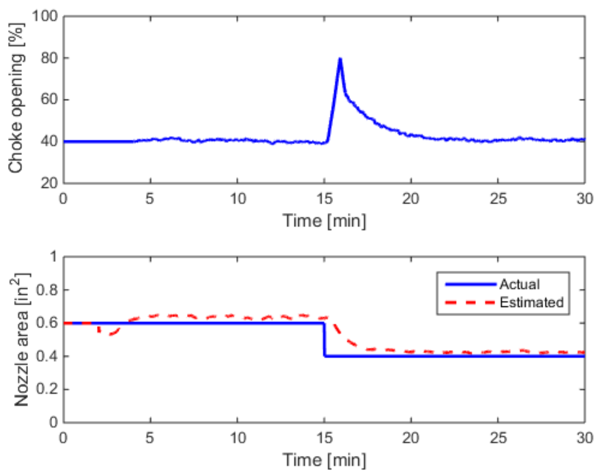

Figure 18. Choke opening and nozzle area for plugged nozzle scenario.

4.5 Pump Efficiency Loss

The pump efficiency loss is simulated through a gradual drop (see bottom plot of **Figure 19**) over a 15-minute period. The system detects this within 2 minutes of the onset of pump degradation, and the event probability peaks at 74% (**Figure 20**). As the pump produces lower volumes per stroke, the standpipe pressure also drops (lower plot of **Figure 21**), as a result of the lower effective flow in rate. Since standpipe pressure control is used, this causes the automatic closing of the choke in order to keep the pressure close to the target by adding back-pressure. The initial choke adjustment is too drastic, which results in a pressure spike seen at the bottom-hole (upper plot of **Figure 21**). Upon detection of the pump efficiency loss, the controller switches to the BHP set point, and the system opens the choke slightly to relieve the extra back-pressure and then gradually closes it in synchronization with the pump efficiency reduction. This allows the system to maintain the BHP close to the target value.

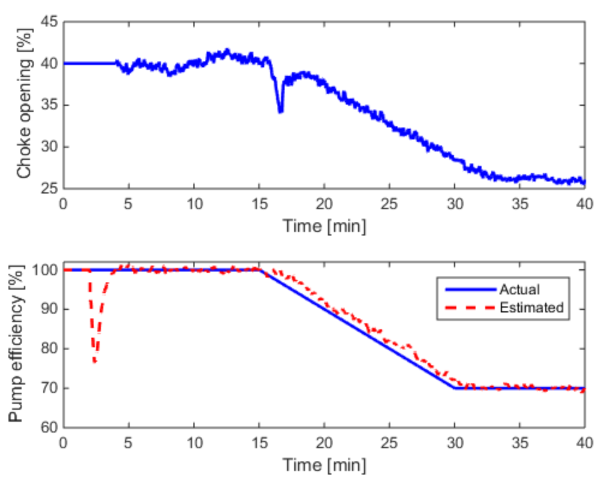

Figure 19. Choke opening and pump efficiency for pump efficiency loss scenario.

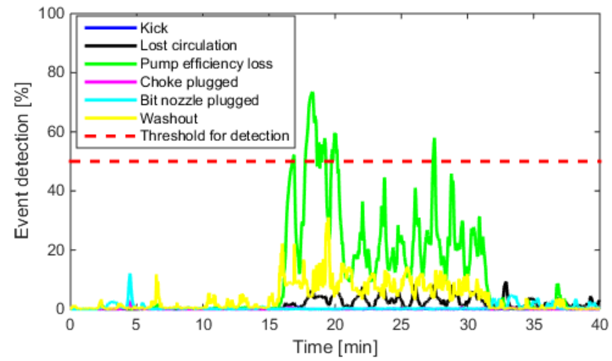

Figure 20. Event detection outputs for pump efficiency loss scenario.

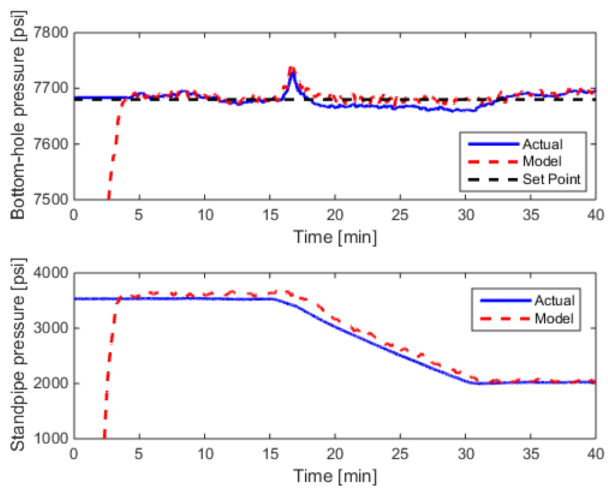

Figure 21. Bottom-hole pressure and standpipe pressure for pump efficiency loss scenario.

4.6 Drill Pipe Washout

For this scenario, we simulate a washout occurring at 3000 ft MD, its size increasing linearly over a 15-minute period. The washout is detected after 3 minutes, with a probability peaking at 68% (**Figure 22).** The initial spike in pump efficiency detection is a result of the similar signatures shared by the two events (decrease in standpipe pressure and flow out), but eventually the system is capable of distinguishing the washout as flow out stabilizes after the transient (bottom plot of Figure **23**). Also, the initial signature of decreasing standpipe pressure (lower plot of **Figure 24**) is masked somewhat by the increase in back-pressure, as the choke is closed to maintain the standpipe pressure target (**Figure 23**). Once again, the control set point is switched to BHP, and the choke opens again to restore the correct amount of back-pressure required to maintain the BHP target. The washout magnitude reaches 160 gpm at its peak, as seen from the difference between pump rate and flow rate through the bit (**Figure 23**). Since the hydraulics model is not re-calibrated to account for the washout (estimating the exact location and magnitude of the washout would require additional downhole sensors), a large discrepancy remains between the modeled and actual pump pressure, but this does not significantly affect the model-predicted BHP, as **Figure 24** indicates. The effective drop in BHP due to the washout is less than 30 psi, which accounts for the reduction in annular friction losses.

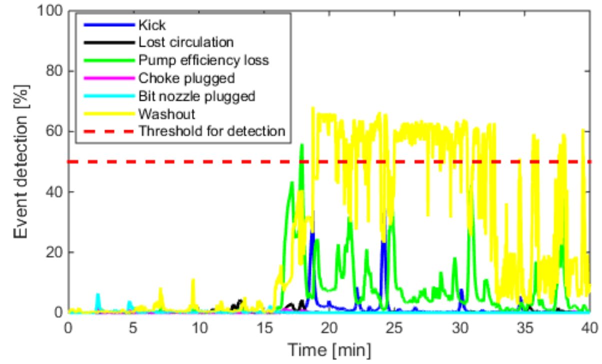

Figure 22. Event detection outputs for washout scenario.

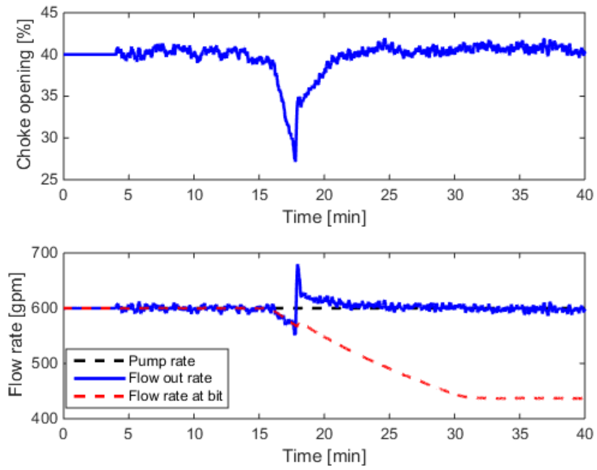

Figure 23. Choke opening and flow rates for washout scenario.

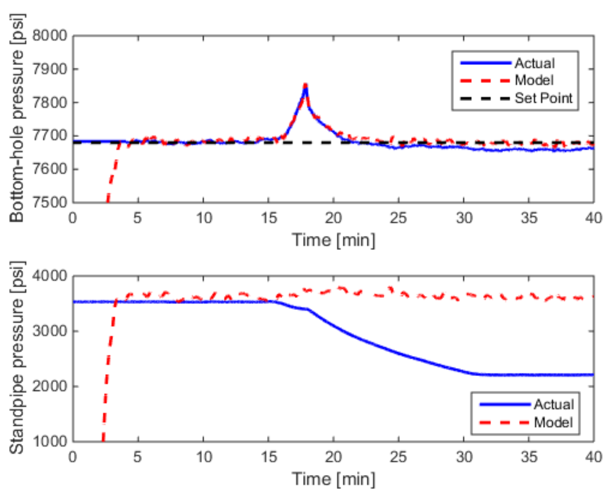

Figure 24. Bottom-hole pressure and standpipe pressure for washout scenario.

4.7 Drill Pipe Connection

The final scenario investigates the controller performance during a connection, aiming to keep a constant BHP target of 7580 psi. To simulate the connection, the pump rate is brought from 600 gpm down to zero in 5 minutes, kept at zero for 7 minutes, and then ramped back to 600 gpm, as per the lower plot of **Figure 25.** The choke is allowed to close completely during the connection, using the trapped back-pressure to compensate for the annular friction once circulation stops. For this task, the modeled BHP value will be used throughout for the pressure controller, as standpipe pressure varies significantly during the pump shut-down and start-up. As **Figure 26** shows, the BHP stays within a 50 psi range of the target during the entire process, with minimal overshoot during pump shut-down and start-up. A back-pressure pump with a separate controller may be used to maintain continuous flow through the choke, and further smoothen out the pressure transients, but this is beyond the scope of this work.

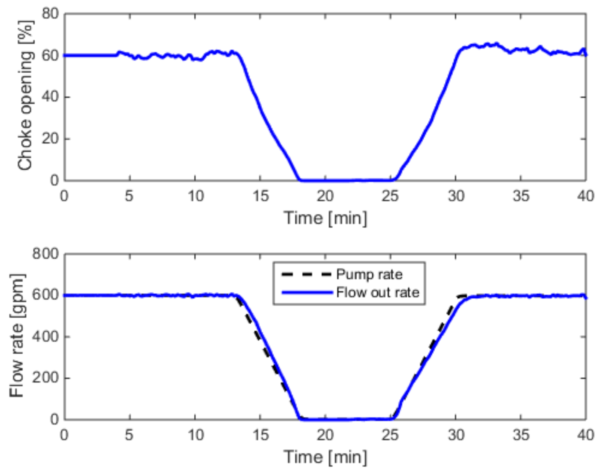

Figure 25. Choke opening and flow rates for connection scenario.

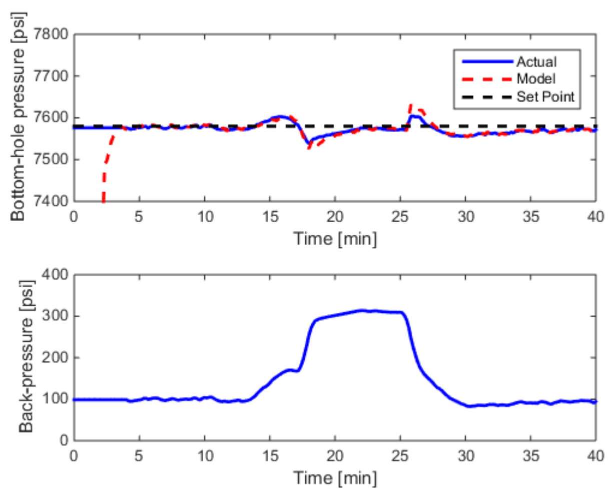

Figure 26. Bottom-hole pressure and back-pressure for connection scenario.

5. Conclusions and Future Work

The conclusions of this paper are summarized below:

- A novel choke control system for Managed Pressure Drilling was developed and tested in a variety of scenarios using advanced simulation software.
- The controller uses a real-time hydraulics model based on a reduced Drift-Flux approach, coupled with parameter estimation algorithms, allowing the system to monitor any change in system conditions and to inform the controller accordingly.
- The controller also includes an event detection system consisting of a Bayesian Network model, which fuses real-time data and predictions from the hydraulics model while encompassing uncertainty in the system representation.
- The controller employs two control modes for the automatic choke operation, as well as advanced logic for set point calculation, enabling the system to select the optimal set points based on the system conditions.
- The full system was tested in seven simulated test scenarios: kick, lost circulation, plugged choke, plugged bit nozzle, pump efficiency loss, drill pipe washout and drill pipe connection events.
- For each scenario, the system was able to hold the downhole pressure close to the specified target, and correctly detect and respond to any adverse conditions in a timely manner.

Future work on this topic should focus on application of the algorithms in field tests as well as making further refinements. Also, investigating more fault scenarios (annular pack-off, borehole enlargement, RCD failure, sensor drift or bias, etc.) may be possible, as well as simulating multiple faults occurring simultaneously (e.g. loss of pump efficiency during a kick or lost circulation event). Implementing additional control laws for main pump and/or back-pressure pump control, and ensuring smooth coordination with the choke controller may be another area of further work.

Acknowledgments

The authors would like to thank Ulf Jakob Aarsnes for assistance with the hydraulics model and control law theory, and Zheren Ma for assistance with the advanced simulator software. Financial support and guidance by the current RAPID (Rig Automation and Performance Improvement in Drilling) sponsor group is also gratefully acknowledged.

Nomenclature

Acronyms

CBHP = *Constant Bottom-Hole Pressure*
CPT = *Conditional Probability Table*
ERD = *Extended Reach Drilling*
MD = *Measured Depth*
MPD = *Managed Pressure Drilling*
RCD = *Rotating Control Device*
TVD = *True Vertical Depth*

Symbols

A_c = *Choke orifice area, m²*
C_b = *Bit nozzle area coefficient*, m^{-4}
C_v = *Choke area coefficient*, m^2
e_p = *Error in pressure tracking, Pa*
$\mathcal{F}$ = *Low-pass filter*
k_P = *Proportional gain*
k_I = *Integral gain*, s^{-1}
M = *Fluid inertia*, kg/m^4
p_c = *Surface back-pressure, Pa*
p_f = *Frictional pressure drop, Pa*
p_g = *Hydrostatic pressure, Pa*
p_s = *Choke downstream pressure, Pa*
p_{st} = *Standpipe pressure, Pa*
q_b = *Volumetric flow rate through bit*, m^3/s
q_c = *Volumetric flow rate through choke*, m^3/s
$q_{g,ex}$ = *Gas expansion rate*, m^3/s
$q_{g,out}$ = *Gas flow rate out*, m^3/s
q_{kick} = *Influx rate*, m^3/s
q_{loss} = *Mud loss rate*, m^3/s
$q_{l,in}$ = *Liquid injection rate*, m^3/s
$q_{l,out}$ = *Liquid flow rate out*, m^3/s
$q_{l,out}^{sp}$ = *Liquid flow rate out set point*, m^3/s
V_a = *Annulus volume*, m^3
Y = *Gas expansion factor*
Z = *Choke opening*

Greek Letters

β = *Drilling fluid bulk modulus, Pa*
γ = *Tuning factor in parameter estimation*
η = *Mud pump volumetric efficiency*
λ = *Tuning factor in parameter estimation*
ρ_l = *Liquid density*, kg/m^3
ρ_g = *Gas density*, kg/m^3
χ_l = *Liquid mass fraction*
χ_g = *Gas mass fraction*

References

1. Aarsnes, U. J, F., Ambrus, A., Di Meglio, F., Vajargah, A. K., Aamo, O.-M., and van Oort, E. (2016a). A simplified two-phase flow model using a quasi-equilibrium momentum balance. International Journal of Multiphase Flow, Volume 83, July 2016, Pages 77-85.
2. Aarsnes, U. J. F., Acıkmese, B., Ambrus, A., and Aamo, O.-M. (2016b). Robust controller design for automated kick handling in Managed Pressure Drilling. Journal of Process Control, Volume 47, November 2016, Pages 46-57.
3. Aarsnes, U. J. F., Ambrus, A., Vajargah, A. K., Aamo, O. M., & van Oort, E. (2015, October). A simplified gas-liquid flow model for kick mitigation and control during drilling operations. In ASME 2015 Dynamic Systems and Control Conference. American Society of Mechanical Engineers.
4. Ahmed, R., Miska, S.Z. (2009). Advanced Wellbore Hydraulics.

In: Aadnoy, B.S. (Ed.), Advanced Drilling and Well Technology. Society of Petroleum Engineers, pp. 191-219.

5. Ambrus, A., Aarsnes, U. J. F., Vajargah, A. K., Akbari, B., & van Oort, E. (2015, December 6). A Simplified Transient Multi-Phase Model for Automated Well Control Applications. International Petroleum Technology Conference. doi:10.2523/IPTC-18481-MS
6. Ambrus, A., Aarsnes, U. J. F., Vajargah, A. K., Akbari, B., & van Oort, E. and Aamo, O.-M. (2016). Real-time estimation of reservoir influx rate and pore pressure using a simplified transient two-phase flow model. Journal of Natural Gas Science and Engineering, Volume 32, May 2016, Pages 439-452.
7. Godhavn, J.-M. (2010, September 1). Control Requirements for Automatic Managed Pressure Drilling System. Society of Petroleum Engineers. doi:10.2118/119442-PA
8. Guner, H. (2009). Simulation Study of Emerging Well Control Methods for Influxes Caused by Bottom-hole Pressure Fluctuations during Managed Pressure Drilling. MS thesis, Louisiana State University, Baton Rouge, Louisiana.
9. Kaasa, G.-O., Stamnes, Ø. N., Aamo, O. M., & Imsland, L. S. (2012, March 1). Simplified Hydraulics Model Used for Intelligent Estimation of Downhole Pressure for a Managed-Pressure-Drilling Control System. Society of Petroleum Engineers. doi:10.2118/143097-PA
10. Koller, D., & Friedman, N. (2009). Probabilistic graphical models: principles and techniques. MIT press.
11. Ma, Z., Vajargah, A. K., Ambrus, A., Ashok, P., Chen, D., van Oort, E., May, R., Macpherson, J. D., Becker, G., Curry, D. A. (2016, September 26). Multi-Phase Well Control Analysis During Managed Pressure Drilling Operations. Society of Petroleum Engineers. doi:10.2118/181672-MS
12. Saeed, S., Lovorn, R., & Arne Knudsen, K. (2012, January 1). Automated Drilling Systems for MPD-The Reality. Society of Petroleum Engineers. doi:10.2118/151416-MS.
13. Santos, H., Leuchtenberg, C., & Shayegi, S. (2003, January 1). Micro-Flux Control: The Next Generation in Drilling Process. Society of Petroleum Engineers. doi:10.2118/81183-MS
14. van Riet, E. J., Reitsma, D., & Vandecraen, B. (2003, January 1). Development and Testing of a Fully Automated System to Accurately Control Downhole Pressure During Drilling Operations. Society of Petroleum Engineers. doi:10.2118/85310-MS